

## DARK MATTER AND THE CHEMICAL EVOLUTION OF IRREGULAR GALAXIES

L. CARIGI, P. COLÍN, AND M. PEIMBERT

Instituto de Astronomía, Universidad Nacional Autónoma de México, Mexico

submitted to the *Astrophysical Journal*

### ABSTRACT

We present three types of chemical evolution models for irregular galaxies: closed-box with continuous star formation rates (SFRs), closed-box with bursting SFRs, and O-rich outflow with continuous SFRs. We discuss the chemical evolution of the irregular galaxies NGC 1560 and II Zw 33, and a “typical” irregular galaxy. The fraction of low-mass stars needed by our models is larger than that derived for the solar vicinity, but similar to that found in globular clusters. For our typical irregular galaxy we need a mass fraction of about 40 % in the form of substellar objects plus non baryonic dark matter inside the Holmberg radius, in good agreement with the results derived for NGC 1560 and II Zw 33 where we do have an independent estimate of the mass fraction in non baryonic dark matter. Closed-box models are better than O-rich outflow models in explaining the C/O and Z/O observed values for our typical irregular galaxy.

*Subject headings:* galaxies: abundances – galaxies: evolution – galaxies: irregular – stars: luminosity function, mass function

### 1. INTRODUCTION

Carigi et al. (1995, hereinafter CCPS) presented a series of models of chemical evolution of irregular galaxies; they concluded that an IMF with a larger fraction of low-mass stars than in the solar vicinity, as well as the presence of a moderate O-rich outflow, were needed to fit a series of observational constraints provided by a “typical” irregular galaxy, these constraints correspond to average values of well observed irregular galaxies. The models were computed based on the yields by Maeder (1992) and under the assumption that no non baryonic matter was present. Recent advances led us to produce a new set of models taking into account the following developments: a) the determination of accurate IMFs for globular clusters based on HST observations, b) the determinations of new yields for massive stars by Woosley, Langer & Weaver (1993) (WLW) and Woosley & Weaver (1995) (WW), c) the determination of the amount of dark matter in several irregular and spiral galaxies, d) better estimates of the H<sub>2</sub> content in irregular galaxies.

In §2 we define the different mass fractions present in an irregular galaxy and their role in chemical evolution models. In §3 we discuss the evidence in favor of a larger fraction of low-mass stars in the IMF than previously adopted for the solar vicinity, consequently we present modified IMFs characterized by a parameter  $r$  also defined in this section. In §4 we present the assumptions adopted for our chemical evolution models. In §5 we present models for two irregular galaxies, NGC 1560 and II Zw 33, for which the amount of non baryonic dark matter is known. In §6 we present the observational properties of a typical irregular galaxy and produce closed-box models with continuous SFRs that reproduce the observational constraints. We have also computed closed-box models with bursts of star formation to compare them with the continuous SFR models. The discussion and conclusions are presented in §7 and §8, respectively.

### 2. DEFINITIONS

We can define the gas mass fraction of a galaxy,  $\mu$ , as

$$\mu = M_{\text{gas}}/M_{\text{total}} = M_{\text{gas}}/(M_b + M_{nb}) \quad (1)$$

where  $M_b$  is the baryonic mass and  $M_{nb}$  is the non baryonic mass (we are defining as “ $M_{nb}$ ” the matter that does not follow the stellar or gaseous mass distribution), often  $M_{nb}$  has been called the dark halo mass.  $M_b$  can be expressed as

$$M_b = M_{\text{gas}} + M_{\text{sub}} + M_{\text{vl}} + M_{\text{rest}} + M_{\text{rem}} \quad (2)$$

where  $M_{\text{sub}}$  is the mass in substellar objects ( $m < 0.1$ , throughout this paper  $m$  is given in solar masses) (we are also defining “ $M_{\text{sub}}$ ” as the baryonic dark matter),  $M_{\text{vl}}$  is the mass of stars in the  $0.1 \leq m < 0.5$  range,  $M_{\text{rest}}$  is the mass of stars in the  $0.5 \leq m \leq 85$  range, and  $M_{\text{rem}}$  is the mass in compact stellar remnants. It is possible to evaluate  $\mu$  observationally from a direct determination of  $M_{\text{gas}}$  and a dynamical determination of  $M_{\text{total}}$ .

To produce a chemical evolution model we need to reach a certain O abundance at a given gas mass fraction of the material that participates in the chemical evolution process,  $\mu_{\text{IMF}}$ , given by

$$\mu_{\text{IMF}} = M_{\text{gas}}/M_b \quad (3)$$

which together with equation (1) yields

$$\mu_{\text{IMF}} = \mu(1 + M_{nb}/M_b) \quad (4)$$

From an observational value of  $\mu$ , but without knowing  $M_{nb}/M_b$ , from equation (4) it follows that we can only derive a lower limit for  $\mu_{\text{IMF}}$ . Note that in O-rich outflow models  $\mu_{\text{IMF}}$  does not include the mass lost in the outflow.

### 3. THE $R$ PARAMETER

#### 3.1. An Initial Mass Function

TABLE 1  
 $r$  VALUES

Object	Ref	$\alpha_1^a$	0.01-85 $M_\odot$	0.01-120 $M_\odot$	0.08-85 $M_\odot$
Solar vicinity	KTG	1.30	1.000	1.000	1.000
Solar vicinity	KTG	1.85	1.512	1.510	1.199
Solar vicinity	KTG	0.70	0.820	0.820	0.883
NGC 6752	FCBRO	1.90, 2.33 <sup>b</sup>	1.879	1.876	1.368
NGC 7099	PCK	2.00	1.812	1.809	1.279
NGC 6397	PCK	1.60	1.202	1.201	1.093

$$^a \text{IMF} \propto \begin{cases} m^{-\alpha_1} & \text{if } m_l \leq m < 0.5, \\ m^{-2.2} & \text{if } 0.5 \leq m < 1.0, \\ m^{-2.7} & \text{if } 1.0 \leq m < m_u. \end{cases}$$

$$^b m^{-1.9} \text{ if } m_l \leq m < 0.27, \quad m^{-2.33} \text{ if } 0.27 \leq m < 0.5.$$

The IMF for the solar neighborhood adopted in this paper is what was called KTG IMF (Kroupa et al. 1993) in CCPS, except that here the upper limit is taken to be 85  $M_\odot$ , and it is given by

$$\xi(m) = \begin{cases} 0.506 m^{-1.3} & \text{if } 0.01 \leq m < 0.5, \\ 0.271 m^{-2.2} & \text{if } 0.5 \leq m < 1.0, \\ 0.271 m^{-2.7} & \text{if } 1.0 \leq m \leq 85, \end{cases} \quad (5)$$

where  $\xi(m)dm$  is the number of stars in the mass interval from  $m$  to  $m + dm$ . This function is extended to a minimum mass of 0.01 to take into account the fraction of dark matter hidden in objects of substellar mass. This function is normalized to one; that is,

$$\int_{m_l}^{m_u} m \xi(m) dm = 1, \quad (6)$$

where  $m_l$  and  $m_u$ , the lower and upper limits, are taken to be 0.01 and 85, respectively, unless otherwise stated.

### 3.2. Chemical Evolution Models and the Value of $r$

An  $r$  value was defined in CCPS as follows

$$r(m_l, m_u) = \frac{\int_{0.5}^{m_u} m \xi(m) dm}{\int_{0.5}^{m_u} m \xi'(m) dm}, \quad (7)$$

where  $m_l$  and  $m_u$  are the low-mass and the high-mass end of the IMF respectively,  $\xi(m)$  is the KTG IMF, and  $\xi'(m)$  is an IMF with different slope in  $m_l \leq m < 0.5$  range (see equation 5 and Table 1);  $r$  depends on  $m_l$  because  $\xi(m)$  and  $\xi'(m)$  are normalized to one (see equation 6).

The chemical evolution models depend on  $r$  because the net yields of the heavy elements, and in particular that of O, decrease when  $r$  increases. (See the definition of net yield in Peimbert, Colín & Sarmiento 1994, and models for different  $r$  values in CCPS).

The closed-box model based on the yields by Maeder (1992) is unable to reproduce simultaneously the  $\mu$ , O, C/O, Z/O, and  $\Delta Y/\Delta O$  values of the typical irregular galaxy studied by CCPS. CCPS were able to reproduce

the observed constraints based on an O-rich outflow model with  $\gamma = 0.23$  and  $r(0.01, 120) = 2.66$ , where  $\gamma$  is the fraction of O produced by SNe that is ejected to the intergalactic medium without mixing with the interstellar gas.

We want to study the effect of using different yields in the models. We will produce closed-box models for different  $r$  values to fit the observational constraints. We will discuss if these  $r$  values are in agreement with the observed IMFs of globular clusters and of the solar vicinity.

### 3.3. Solar Vicinity

We will study two problems: the  $r$  values determined for different IMFs and the effect of the yields by Maeder and WLW & WW on the  $M_{sub}$  value for chemical evolution models of the solar vicinity.

In Table 1 we present  $r$  values for different mass ranges and for different values of the slope for the low-mass range,  $\alpha_1$ , given by  $\text{IMF} \propto m^{-\alpha_1}$  for  $m_l \leq m < 0.5$ ; we have adopted the IMF slopes given by KTG for  $m \geq 0.5$ . In Table 2 we present the average mass of the objects in the IMF from  $m_x$  to  $m_u$ , when  $m_x = m_l = 0.01$  we include all objects in the IMF and when  $m_x = 0.1$  we include only stellar objects in the IMF.

The KTG simulations of star-count data reach the maximum confidence when the scale height for their model reaches 270 pc; in this case  $\alpha_1 = 1.3$ . Based on their model KTG suggest for the solar vicinity that  $0.70 < \alpha_1 < 1.85$ , for the  $0.08 \leq m < 0.5$  range. We adopted  $\alpha_1 = 1.3$  as the preferred value, and for this value we define  $r = 1$  for the three mass ranges presented in Table 1 (see the first line of this table).

We present three mass ranges in Table 1 for the following reasons: Maeder (1992), and WLW (1993) use  $m_u$  equal to 120 and 85 respectively, while CCPS and in this paper we have adopted  $m_l = 0.01$ , in the last column we present the lower mass included by KTG,  $m_l = 0.08$ .

Carigi (1996) computed a chemical evolution model of the solar neighborhood with  $M_{nb} = 0$  based on the yields by Maeder (1992) adopting the KTG IMF for the  $0.01 \leq m \leq 120$  range. For this model the mass fraction in

substellar objects amounts to 15.1 % and the present day gas fraction is 0.15 in agreement with the data (0.05–0.20, Tosi 1996).

We have computed a model for the solar neighborhood under the same assumptions as those adopted by Carigi (1996), but based on the yields by WLW and WW, and adopted a  $0.01 \leq m \leq 85$  mass range ( $r = 1$ ). We obtain for this model a mass fraction in substellar objects of 14 % and the present day gas fraction is 0.07, also in agreement with the observations (Tosi 1996).

Both models of the solar vicinity could accommodate an additional modest amount of substellar objects or non baryonic dark matter and still reproduce the observed abundances and the  $\sigma_{gas}/\sigma_{total}$  value.

If there is a significant fraction of non baryonic dark matter that does not participate in the chemical evolution process, it has to be subtracted from  $M_{total}$  increasing the value of  $\mu_{IMF}$ . Therefore to reach the observed abundances with lower gas consumption the IMF needs to have a larger fraction of massive stars, and if we keep the KTG slope for massive stars constant we need to reduce the fraction of low-mass stars in the model, and consequently  $r$  values smaller than one.

On the other hand, if  $M_{total}$  is larger than the observed value adopted by us, and if this difference is due to a greater mass fraction in substellar objects in the solar vicinity, then the  $\mu_{IMF}$  would become smaller and the model would need a higher gas consumption and  $r$  values higher than one to be able to reproduce the observed abundances.

### 3.4. Globular Clusters

Based on HST observations Ferrano et al. (1997, hereinafter FCBRO) determined the mass function for the lower main sequence of the globular cluster NGC 6752 ( $Z = 0.03 Z_{\odot}$ ). They found  $x$  values of 0.90 and 1.33 for the mass ranges  $0.15 - 0.30 M_{\odot}$  and  $0.25 - 0.55 M_{\odot}$ , respectively, where  $\xi'$  is proportional to  $m^{-(1+x)}$ . Therefore we have adopted for NGC 6752:

$$\xi'_{6752}(m) \propto \begin{cases} m^{-1.9} & \text{if } m_l \leq m < 0.27, \\ m^{-2.33} & \text{if } 0.27 \leq m < 0.5, \\ m^{-2.2} & \text{if } 0.5 \leq m < 1.0, \\ m^{-2.7} & \text{if } 1.0 \leq m \leq m_u. \end{cases} \quad (8)$$

Note that to derive an  $r$  value we need to define the IMF in the  $m_l$ - $m_u$  range and that for  $m \geq 0.5$  we are adopting KTG for all globular clusters.

Also based on HST observations Piotto, Cool, & King (1997, hereinafter PCK) have determined the mass function of four globular clusters. Three of them have very similar mass functions: NGC 6341, NGC 7078 and NGC 7099. Based on the mass luminosity relation by D'Antona and Mazzitelli (1995) PCK derive for NGC 7099 that  $x = 1.0$  for masses below  $0.4 M_{\odot}$ . Consequently, we have adopted for NGC 7099:

$$\xi'_{7099}(m) \propto \begin{cases} m^{-2.0} & \text{if } m_l \leq m < 0.5, \\ m^{-2.2} & \text{if } 0.5 \leq m < 1.0, \\ m^{-2.7} & \text{if } 1.0 \leq m \leq m_u. \end{cases} \quad (9)$$

For the same mass range, and the same mass luminosity relation PCK find  $x = 0.6$  for NGC 6397. They suggest that the lower value of  $x$  derived for NGC 6397, relative

to the other three clusters, could be due to selective loss of low-mass stars by evaporation and tidal shocks.

In Table 1 we present the NGC 6752, NGC 7099 and NGC 6397  $r$  values for the different mass ranges considered. By comparing the  $r$  values for different mass ranges it is found that the effect on  $r$  introduced by changing the upper mass end from 120 to 85  $M_{\odot}$  is negligible. Moreover, it is also found that the  $r$  values for NGC 6752 and NGC 7099 are significantly higher than for the solar vicinity. This result implies that the fraction of low-mass stars is higher for globular clusters than for the solar vicinity, and might imply that the fraction of substellar objects is higher also.

## 4. CHEMICAL EVOLUTION MODELS

All the models in this paper reproduce at least two observational constraints: the O abundance by mass in the interstellar medium (ISM), and  $\mu$ . In addition each model predicts different element abundance ratios by mass that can be compared with other observational constraints.

We computed three types of models: closed-box with continuous SFRs, closed-box with bursting SFRs, and O-rich outflow with continuous SFRs. The assumptions adopted in our models are:

- a) The initial composition of the gas is primordial:  $Y_0 = 0.23$ ,  $Z_0 = 0.00$ .
- b) We have computed models for three galaxy ages,  $t_g$ : 0.1, 1.0, and 10.0 Gyr
- c) The star formation rate is proportional to the gaseous mass,  $SFR = \nu M_{gas}$ . The efficiency,  $\nu$ , is mainly determined by the need to reach  $\mu_{IMF}$  at the age of the model. For a continuous SFR  $\nu$  is constant in time. On the other hand, when we consider a bursting SFR

$$\nu = \begin{cases} \text{constant} & \text{if } t_j \leq t < t_j + 40 \text{ Myr}, \\ 0 & \text{if } t_j + 40 \text{ Myr} \leq t \leq t_{j+1}, \end{cases} \quad (10)$$

where  $t_j = (t_g - 0.2) \frac{(j-1)}{(n-1)}$  Gyr is the burst starting time,  $n$  is the total number of bursts, and  $1 \leq j \leq n$ .

d) We have adopted several IMFs (see §3). For  $m \geq 0.5$  all of them have the same slopes as those given by KTG. The  $r(0.01, 85)$  value is varied until the desired oxygen abundance is obtained. This  $r(0.01, 85)$  value corresponds to a unique IMF with a slope for stars with  $m < 0.5$  denoted by  $\alpha_1$ . In what follows  $r$  corresponds to the 0.01-85 mass interval unless otherwise noted.

e) We drop the instantaneous recycling approximation, IRA, and assume that the stars eject their envelopes after leaving the main sequence. The main sequence lifetimes are taken from Schaller et al. (1992). The possible reduction of the O yields of massive stars due to the production of black holes as suggested by Maeder (1992) has not been considered.

f) We have used the stellar yields and remnant masses due to: i) Renzini & Voli (1981) for  $1.0 \leq m \leq 8.0$  ( $\alpha = 1.5$ ,  $\eta = 1/3$ ); ii) WW for  $11 \leq m \leq 40$  (models "B" for 30, 35 and 40  $M_{\odot}$ ); iii) WLW for  $m = 60$  and  $m = 85$ . We also consider the changes in the stellar yields due to the stellar initial metallicity. Only massive stars, those with  $m > 8$ , enrich the ISM with oxygen.

g) For SNIa we have taken into account the yields by Nomoto, Thielemann, & Yokoi (1984, model W7). Only a fraction of binary stars, in the  $3 \leq m_1 + m_2 \leq 16$  range,

TABLE 2  
 $\langle m \rangle$  VALUES

$\alpha_1^a$	0.1-85 $M_\odot$	0.1-120 $M_\odot$	0.01-85 $M_\odot$	0.01-120 $M_\odot$	0.08-85 $M_\odot$
1.30	0.501	0.503	0.194	0.195	0.452
1.85	0.391	0.393	0.074	0.074	0.335
0.70	0.626	0.629	0.429	0.431	0.593
1.90, 2.33	0.345	0.346	0.062	0.062	0.293
2.00	0.364	0.366	0.058	0.058	0.307
1.60	0.440	0.441	0.116	0.116	0.386

<sup>a</sup> As in Table 1.

become SNIa; where  $2.2 \leq m_1 \leq 8.0$  and  $0.8 \leq m_2 \leq 8.0$ . We have determined such fraction by fitting the observed solar Fe abundance.

h) In models with outflow of O-rich material we assume that a fraction,  $\gamma$ , of the mass expelled by type II SNe is ejected to the intergalactic medium without mixing with the ISM. The WW yields have been computed without considering stellar winds, therefore the ejected mass during a SN explosion is equal to the initial mass minus the stellar remnant.

### 5. NGC 1560 AND II ZW 33

There are two irregular galaxies with good O/H values for which  $\mu_{IMF}$  can be determined: NGC 1560 and II Zw 33, also known as *Markarian 1094*. For these two galaxies we can compute closed-box models for different ages, each model characterized by an  $r(0.01, 85)$  value, which corresponds to a specific IMF.

#### 5.1. $\mu_{IMF}$ and O/H

From the studies of the rotation curves of a few dwarf irregular galaxies it is found that they are dominated by non baryonic dark matter (e.g., Burlak 1996, Salucci & Persic 1997), some of them well within the core of the mass distribution (e.g., Moore 1994). In general most of the  $M_{nb}$  is present outside the Holmberg radius. Unfortunately, for most of these non baryonic dominated galaxies, for which a rotation curve is available, chemical abundance determinations do not exist. From the very reduced group for which rotation curves as well as oxygen abundances are available we have extracted NGC 1560 and II Zw 33 to build chemical evolution models. For these galaxies  $M_{gas}$ ,  $M_b$ , and consequently  $\mu_{IMF}$  are known and are presented in Table 3 (see Walter et al. 1997 and Broeils 1992).

The O/H gaseous value for NGC 1560 comes from Richer & McCall (1995) and for II Zw 33 comes from Esteban & Peimbert (1995). To derive the O abundances by mass we have considered the contribution of O expected to be in dust grains (0.04 dex) and the effect of temperature variations over the observed volume (0.16 dex); consequently we have added 0.2 dex to the gaseous values derived under the assumption of a constant temperature distribution inside the H II regions (see CCPS and references therein).

#### 5.2. Closed-box Models with Continuous SFRs for NGC 1560 and II Zw 33

Closed-box models for NGC 1560 and II Zw 33 have been computed under the assumptions presented in §4. The models reproduce  $\mu_{IMF}$  and the O abundance by mass shown in Table 3.

In Table 4 we present three models computed for NGC 1560 with continuous SFRs. Each line of this Table represents a different model. For each age we find a unique  $r(0.01, 85)$  value. Columns 3 to 6 show the mass fractions defined in equations (1) and (2). The C/O,  $\Delta Y/\Delta O$ , and Z/O ratios are presented in columns 7 to 9; in all tables C, O, Y and Z are given by mass.

The models with  $\gamma = 0.00$  and  $M_{nb} = 0.0$  for II Zw 33 are presented in Tables 5 and 6, for these models  $\mu_{IMF} = 0.29$ . From these models we note that: a)  $r$  increases with model age because a larger fraction of stars have enriched the ISM with heavy elements and the model needs to reduce  $M_{rest}$  (columns 5 and 6 of Tables 4 and 5, respectively); b) if  $r$  increases,  $\alpha_1$  increases and  $M_{sub}$  becomes higher; c)  $M_{vl}$  changes little with age; d) despite the fact that  $M_{rest}$  decreases with age  $M_{rem}$  grows with age because the fraction of stars that have had time to end their evolution is higher; e) for NGC 1560  $M_{sub} + M_{nb} \sim 61\%$  and  $r \sim 1.73$  while for II Zw 33,  $M_{sub} + M_{nb} \sim 43\%$  and  $r \sim 2.75$ , at 10 Gyr; f) the 1.0-Gyr and 10-Gyr models predict C/O and Z/O ratios higher than those determined observationally for our typical irregular galaxy (see Tables 9); g) the 0.1-Gyr models reproduce well the observed C/O and Z/O ratios but predict lower  $\Delta Y/\Delta O$  values than observed.

#### 5.3. Additional Models for II Zw 33

There is no compelling observational evidence for large systematic IMF variations in galaxies for  $m > 1.0$  (e.g., Kennicutt 1998 and references therein). Therefore it is possible that the IMF could be the same everywhere for  $m < 1.0$ . This would imply a unique  $r$  value for all objects. Therefore we will explore if it is possible to produce chemical evolution models for II Zw 33 with  $r = 1.8$ , the average value for NGC 6752, NGC 7099, and NGC 1560 ( $t_g = 10$  Gyr). There are two groups of models that satisfy the  $r = 1.8$  requirement; closed-box models with  $M_{nb} \neq 0.0$  and O-rich outflow models with  $M_{nb} = 0.0$ . In what

TABLE 3  
PROPERTIES OF NGC 1560 AND II Zw 33

Galaxy	$\log(M_{total}/M_{\odot})$	$\log(M_{gas}/M_{\odot})$	$\log \mu$	$\log \mu_{IMF}$	$10^3 O$
NGC 1560	9.83	9.20	-0.63	-0.34	2.03
II Zw 33	9.71	9.17	-0.54	-0.54	1.93

TABLE 4  
PROPERTIES OF SELECTED GALAXIES

Galaxy	$\log(M_{total}/M_{\odot})$	$\log(M_{gas}/M_{\odot})$	$\log \mu$	$Y$	$10^3 O^a$
I Zw 18	8.26	8.21	-0.05	0.230	0.317
UGC 4483	8.07	7.95	-0.12	0.239	0.639
Mrk 600	8.88	8.76	-0.12	0.240	1.967
SMC	9.12	8.71	-0.41	0.237	2.268
II Zw 40 <sup>b</sup>	9.46	8.62	-0.84	0.251	2.672
IC 10	10.03	9.74	-0.29	0.240	2.775
II Zw 70	9.14	8.67	-0.47	0.250	3.287
NGC 6822	9.23	8.31	-0.92	0.246	3.305
LMC	9.78	8.88	-0.90	0.250	4.133
NGC 4449	10.91	9.63	-1.28	0.251	4.526
average	9.29	8.75	-0.54	0.243	2.589

<sup>a</sup>The O gaseous values have been multiplied by 1.58 (0.2 dex, see text).

<sup>b</sup>Values quoted for the northern cloud. Molecular and ionized hydrogen is added.

TABLE 5  
MODELS FOR NGC 1560<sup>a</sup>

$t_g$ (Gyr)	$r$	$M_{sub}(\%)$	$M_{vl}(\%)$	$M_{rest}(\%)$	$M_{rem}(\%)$	C/O	$\Delta Y/\Delta O$	Z/O
0.1	1.471	8.9	8.7	9.9	0.2	0.167	2.844	1.842
1.0	1.615	10.6	8.8	7.5	0.8	0.292	3.678	2.268
10.0	1.727	12.0	9.0	4.5	2.2	0.324	4.167	2.429

<sup>a</sup> $M_{sub} + M_{vl} + M_{rest} + M_{rem} + M_{gas} + M_{nb} = 100.0\%$ , with  $M_{gas} = 23.4\%$ ,  $M_{nb} = 48.9\%$ , and  $\mu_{IMF} = 0.46$

follows we will explore these two possibilities further.

### 5.3.1. Closed-box Models with $M_{nb} \neq 0$

In Tables 5 and 6 we present the main characteristics of models with  $r = 1.8$  and  $M_{nb} \neq 0.0$  for II Zw 33. The two main differences between the models with  $r = 1.8$  and those with  $r > 2.5$  are that, as expected,  $M_{sub}$  decreases and  $M_{nb}$  increases with decreasing  $r$ . The increase in  $M_{nb}$  implies an increase in  $\mu_{IMF}$ . Alternatively the changes in the C/O,  $\Delta Y/\Delta O$ , and Z/O values are negligible. These models would imply that the  $M_{nb}$  determination by Walter et al. (1997) is not correct.

### 5.3.2. O-rich Outflow Models with $M_{nb} = 0$

We have produced O-rich outflow models ( $\gamma \neq 0.00$ ) for II Zw 33 with  $r = 1.8$  and  $M_{nb} = 0.0$  (see Tables 5 and 6). The O-rich outflow models predict C/O,  $\Delta Y/\Delta O$ , and Z/O values higher than the closed-box models (see Table 6). The C/O and Z/O values are not known for II Zw 33; our models predict that if O-rich outflows have been important during the evolution of this object its C/O and Z/O values should be considerably higher than those observed in other irregular galaxies (see §7.2).

## 6. A TYPICAL IRREGULAR GALAXY

For NGC 1560 and II Zw 33 we have only  $\mu_{IMF}$ ,  $M_{nb}$ , and O as observational constraints; these constraints are not enough to decide if O-rich outflows have been present in these objects. We have decided to model a typical irregular galaxy because for it we can use average observational values for  $\mu$ , O, C/O,  $\Delta Y/\Delta O$ , and Z/O, derived from a set of well observed irregular galaxies; these observational constraints will permit us to address the issue of the importance of O-rich outflows for the evolution of the typical dwarf irregular galaxy.

In what follows we will estimate the general properties of a typical irregular galaxy. We will use the same set of galaxies that was used by CCPS. These galaxies were chosen because their properties are well known, in particular the chemical composition of their gaseous content.

For the irregular galaxies in the CCPS sample we do not have a  $\mu_{IMF}$  value because we do not know which is the contribution of the halo dark matter,  $M_{nb}$ , to  $M_{total}$ . Therefore the observed  $\mu$  value is a lower limit to  $\mu_{IMF}$  (see equation 4).

### 6.1. The $\mu$ Value

The  $\mu$  value depends on the  $M_{gas}$  to  $M_{total}$  ratio. We will revise the  $M_{gas}$  and  $M_{total}$  values adopted by CCPS for each galaxy and the new adopted values will be presented in Table 7.

CCPS neglected the contribution of  $H_2$  to  $M_{gas}$  due to the low CO content of the irregular galaxies. Nevertheless, there are observational and theoretical considerations that favor a CO-to- $H_2$  conversion factor,  $X_{CO-H_2}$ , that increases for systems of lower metallicity (Maloney & Black 1988; Wilson 1995; Arimoto, Sofue, & Tsujimoto 1996). Therefore we can not exclude the possibility of having low-metallicity irregular galaxies with a relatively high molecular hydrogen content.

The  $H_2$  mass estimated for II Zw 40 by Tacconi & Young (1987), for NGC 6822 by Israel (1997), and adopted for II

Zw 33 by Walter et al. (1997) is about 10 % of H I mass. Consequently, we will multiply the H I + He I gaseous mass of irregular galaxies by a factor of 1.1 to take into account the contribution due to  $H_2$ , with the exception of I Zw 18, and UGC 4483, where no such correction will be applied (Carigi & Peimbert 1998).

Madden et al. (1997) recently estimated an unusually high  $H_2$  column density (a factor of five that of H I) in three regions of IC 10, their result is based on [C II] 158 micron observations and an argument of thermal balance. If this result is applied to the whole galaxy one finds that  $\mu = 1.2$  which is impossible since by definition  $\mu$  has to be smaller than 1. We consider that there is no room for such high amounts of  $H_2$  in dwarf irregular galaxies (see also Lequeux 1996).

To produce a homogeneous set of  $\mu$  values we need to estimate  $M_{total}$  at a given distance from the galactic center. Wherever possible we have chosen the Holmberg radius,  $R_H$ , because most of the gas and stars are inside it, for larger radii  $M_{nb}$  becomes larger and  $\mu$  becomes smaller deviating more from  $\mu_{IMF}$ .

Based in part on the previous discussion we have introduced the following changes to Table 1 of CCPS and have generated the  $M_{total}$  and  $M_{gas}$  values of Table 7: a) we have added a 10 % to the H I + He I gaseous mass to consider the  $H_2$  contribution for all galaxies except for II Zw 40, where  $H_2$  is explicitly taken by Tacconi & Young (1987), and I Zw 18 and UGC 4483, where we are assuming a null  $H_2$ ; b) we have adopted a Hubble constant of  $H_0 = 100h$  kms Mpc<sup>-1</sup> with  $h = 0.65$ , while CCPS adopted  $h = 0.70$ , errors in the distance,  $d$ , will alter  $\mu_{IMF}$  because  $M_{gas} \propto d^2$  while  $M_{total} \propto d$ ; c) we have revised for each galaxy the determination of  $M_{total}$ . The discussion on the  $M_{total}$  and  $\mu$  determinations for each galaxy follow.

I Zw 18.— The total mass within  $R_H$  (Staveley-Smith, Davies, & Kinman 1992, hereinafter SDK) give a ratio of  $M_{gas}$  to  $M_{total}$  greater than one. On the other hand, assuming that the high radial velocity gradient is due to rotation, Petrosian et al. (1997) derive a total mass (within a radius of 0.48 kpc) higher than that derived by SDK. The difference is due to the higher rotational velocity estimated by Petrosian et al.. Our  $M_{total}$  and  $M_{gas}$  values are those adopted by Carigi & Peimbert (1998), which are a compromise between the values given by SDK and Petrosian et al.. Incidentally, the  $\mu$  value adopted here is close to that adopted by CCPS.

UGC 4483.— There are two determinations of  $M_{total}$ , one by SDK and another by Lo, Sargent, & Young (1993), which together with the  $M_{gas}$  derived by SDK yield an average  $\mu$  value of 0.76. The radius at which  $M_{total}$  is derived, 1.42 kpc (putting UGC 4483 at the distance given by SDK but with  $h = 0.65$ ), is close to its  $R_H = 1.28$  kpc (SDK).

Mrk 600.— We adopted as the total mass within  $R_H$  that derived by SDK but assuming an  $h = 0.65$ .

SMC, LMC, & II Zw 40.— These three galaxies have a total mass derived within a radius that is lower than  $R_H$ , being II Zw 40 the extreme case. This is not a problem as long as  $\mu$  does not suffer a significant change when going from this radius to  $R_H$ . The radius at which the total mass of SMC is derived (Hindman 1967) is close to its  $R_H$  (Balkowski, Chamaraux, & Weliachew 1978), therefore we

TABLE 6  
ABUNDANCE RATIOS FOR II Zw 33

$t_g$ (Gyr)	$r$	$\gamma$	C/O	$\Delta Y/\Delta O$	Z/O
0.1	2.502	0.00	0.169	3.011	1.884
	1.800	0.00	0.168	2.890	1.852
	1.800	0.29	0.170	3.204	1.939
1.0	2.632	0.00	0.311	3.789	2.317
	1.800	0.00	0.294	3.695	2.273
	1.800	0.33	0.383	4.419	2.592
10.0	2.750	0.00	0.328	4.247	2.447
	1.800	0.00	0.325	4.173	2.429
	1.800	0.38	0.425	5.284	2.856

would not have expected a very different  $\mu$  value if  $M_{total}$  had been determined inside  $R_H$  (we are also assuming that the contribution from the gas beyond  $R_H$  is negligible). As the distance determined by Welch et al. (1987) of 61 kpc has now been used, as opposed to 70 kpc, its  $M_{total}$  and  $M_{gas}$  values have changed accordingly. On the other hand, according to Kunkel, Demers, & Irwin (1996) most of the mass of the LMC is located within the inner 5 deg, we are thus not making a big mistake by using the  $\mu$  associated to the inner region of 4.2 deg (Lequeux et al. 1979); apparently there is no massive dark halo in LMC (Kunkel et al. 1997). The H I core of II Zw 40 was studied by Gottesman & Weliachew (1972) and its corresponding  $\mu$  was adopted by CCPS from Lequeux et al.. From the  $M_{total}$  values derived by Brinks & Klein (1988), we find  $\mu$  value of 0.14 for the northern cloud of II Zw 40 (see Table 7). This low value of  $\mu$  might imply the presence of a significant amount of dark matter.

IC 10.— The Keplerian estimate of  $M_{total}$  (Shostak 1974) was derived within a radius which is very close to  $R_H$  ( $R_H=4.0$  kpc, if the distance to the galaxy is taken to be 3 Mpc). Recent determinations of the distance to IC 10 put it close to 1 Mpc (e.g., Wilson et al. 1996). This value contrasts with the 3 Mpc adopted by Lequeux et al. from Sandage & Tammann (1975). We have adopted 1.5 Mpc and at this distance  $\mu = 0.51$ .

II Zw 70 & NGC 6822.— The total masses of these two galaxies are derived within a radius which is greater than their  $R_H$  values by about a factor of two (Balkowski et al. 1978; Gottesman & Weliachew 1977). By using these  $M_{total}$  values, we may be underestimating the value of  $\mu$  as compared with the values derived for other galaxies in the sample. A very detailed modeling of the rotation curve of these two galaxies is needed to know the contribution of a dark halo to the total mass.

NGC 4449.— The total mass of this galaxy, within a radius of 37 kpc (by far greater than its optical radius) has been estimated recently by Bajaja, Huchtmeier, & Klein (1994). Its  $\mu = 0.052$  is considerably lower than those usually estimated for dwarf irregular galaxies, in particular, lower than the other galaxies of our sample. The rotation curve indicates the presence of dark matter in its extended

H I halo but, as in the case of NGC 6822 and II Zw 70, a very detailed modeling of its rotation curve is still needed.

It is interesting to note that the mean  $\mu$  value presented in Table 7 differs only by 2 % from the mean  $\mu$  value obtained by CCPS.

## 6.2. $O$ , C/O, $\Delta Y/\Delta O$ , and Z/O

Columns 5 and 6 of Table 7 present the helium and the oxygen abundances by mass, the data are the same as those presented by CCPS. In the last two lines of Tables 9 and 11 we present the C/O,  $\Delta Y/\Delta O$ , and Z/O values derived by CCPS from their sample of irregular galaxies.

More recent determinations of He abundances permit to derive other  $\Delta Y/\Delta O$  values. From the data of Izotov, Thuan, & Lipovetski (1997) on extragalactic H II regions it is obtained that  $\Delta Y/\Delta O = 3.1 \pm 1.4$ . Based on observations by many authors Olive, Steigman, & Skillman (1997) obtain a pregalactic helium abundance,  $Y_p$ , of  $0.234 \pm 0.002$ , alternatively Izotov et al. find  $Y_p = 0.243 \pm 0.003$ . By adopting  $Y_p = 0.240 \pm 0.006$  and combining this value with the Y and O abundances of the galactic H II region M17, that amount to  $0.280 \pm 0.006$  and  $(8.69 \pm 1.3) \times 10^{-3}$ , respectively (Peimbert, Torres-Peimbert, & Ruiz 1992), it follows that  $\Delta Y/\Delta O = 4.6 \pm 1.1$ . We have added 0.08 dex to the gaseous O abundance to consider the fraction of O atoms embedded in dust (Esteban et al. 1998). Finally, from fine structure in the main sequence based on Hipparcos parallaxes Pagel & Portinari (1998) obtain that  $\Delta Y/\Delta O = 5.6 \pm 3.6$ . These three  $\Delta Y/\Delta O$  values are in good agreement with the value presented in Tables 9 and 11.

## 6.3. *Closed-box Models with Continuous SFRs*

The properties of the typical irregular galaxy were obtained from the galaxies presented in Table 7 and are given in the last row of this table.

We have computed closed-box models with continuous SFRs and different ages for the typical irregular galaxy. All the models reproduce the observational constraints,  $\mu = 0.288$  and  $O = 2.589 \times 10^{-3}$ . For the typical irregular galaxy we do not know the amount of  $M_{nb}$ , therefore the observed  $\mu$  value is a lower limit to  $\mu_{IMF}$ . Consequently,

we have computed models for a range of  $r(0.01, 85)$  values; we think it is unlikely that the  $r$  value is smaller than one (see Table 1), and  $r_{max}$  is the value for  $M_{nb} = 0.0$ ,  $r$  can not be higher than  $r_{max}$  because  $M_{nb}$  would become negative. In Table 8 we present the model results for the different mass fractions defined in this paper.

The distributions of  $M_{sub}$  and  $M_{nb}$  for different  $r(0.01, 85)$  values are plotted in Figure 1. From this figure it can be seen that  $M_{sub}$  increases with  $r$  and  $M_{nb}$  decreases with  $r$ . The increase of  $M_{sub}$  with  $r$  is due to an increase of the slope of the low-mass end of the IMF with  $r$ . The decrease of  $M_{nb}$  with  $r$  is due to the lower efficiency in the O production and therefore to the decrease of  $\mu_{IMF}$  (see Table 8 and equation 4). Furthermore for a given  $r$  value  $M_{sub}$  decreases with the age of the model while  $M_{nb}$  increases with it.

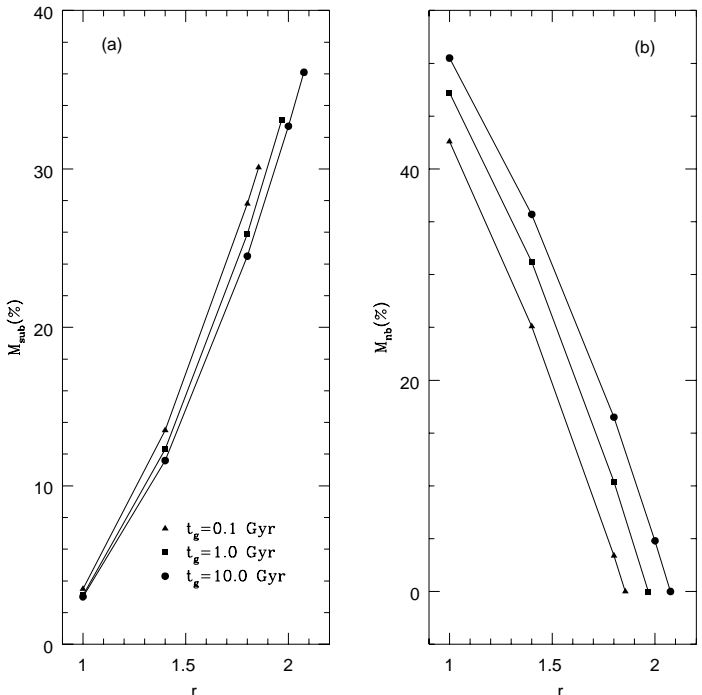


FIG. 1.— Mass fractions of (a) substellar objects,  $M_{sub}$ , and of (b) non baryonic dark matter,  $M_{nb}$ , for different  $r(0.01, 85)$  values. The data correspond to closed-box models with continuous SFRs for different ages of the typical irregular galaxy (see Table 8).

In Table 9 we present the predicted abundance ratios by our closed-box models with continuous SFRs, the predicted abundance ratios by CCPS, and the observed ratios. From this table it can be seen that: a) the predicted abundance ratios for a given model age are almost independent of  $r$ ; b) the predicted ratios increase with model age due to the production of  $Y$  and  $C$  by intermediate mass stars, while  $O$  is produced only by massive stars; c) the  $C/O$  and  $Z/O$  values point to models with ages not older than one Gyr, while the  $\Delta Y/\Delta O$  value indicates older ages. d) our models predict considerably larger values for  $C/O$ ,  $\Delta Y/\Delta O$ , and  $Z/O$  than the models by CCPS, this result is due to the difference between the yields by WLW & WW

and those by Maeder (1992).

Our sample in Table 7 was chosen to have a large spread in  $Y$  and  $O$  to derive a meaningful  $\Delta Y/\Delta O$  value, but our sample is not completely homogeneous because the  $O$  abundances for I Zw 18 and UGC 4483 are very small and the  $M_{total}$  for NGC 4449 was estimated from observations at distances far away from  $R_H$ . To have a more homogeneous sample we can eliminate the three objects in Table 7 that deviate most from the average  $\mu$  and  $O$  values: I Zw 18, UGC 4483, and NGC 4449. For this reduced sample we obtain the following average quantities:  $\log \mu = -0.56$  and  $10^3 O = 2.915$ , in very good agreement with the values adopted for the typical irregular galaxy. Moreover, the chemical evolution models computed to adjust the average values of the reduced sample are very similar to those computed for the typical irregular galaxy.

#### 6.4. Closed-box Models with Bursting SFRs

The presence of old populations in many of the dwarf irregular galaxies in the local group indicates that star formation started  $\sim 10$  Gyr ago (e.g., Mateo 1998; Pagel & Tautvaišienė 1998). The nature of the star formation histories in these galaxies is diverse (e.g., Mateo 1998). The most massive dwarf irregular galaxies appear to have had a continuous SFR, while ordinary dwarf irregular galaxies appear to have undergone a gasping SFRs (e.g., Tosi 1998). It is interesting then to see if by changing the continuous nature of the SFR to a discontinuous one (bursting), our results presented in §6.3 change drastically.

Figure 2 shows in six panels the evolution of: the SFR,  $\mu_{IMF}$ ,  $O$ ,  $C/O$ ,  $\Delta Y/\Delta O$ , and  $Z/O$ . The model is for  $t_g = 1.0$  Gyr and has three bursts each lasting 40 Myr. The behavior of  $O$ ,  $C/O$ ,  $\Delta Y/\Delta O$ , and  $Z/O$  are as expected. The oxygen abundance increases suddenly during each burst and then stays constant in the quiescent phase. On the other hand,  $C$ ,  $Y$  and  $Z$  increase during the quiescent phase because they are also produced by intermediate mass stars. There is a period of time after the second or third burst in which these ratios decrease because the growth rate of the  $O$  abundance is higher than those of  $C$ ,  $Y$ , and  $Z$ . The spike in the  $C/O$ ,  $\Delta Y/\Delta O$ , and  $Z/O$  values at the beginning of the model is due to the  $C$  and  $Y$  production in very massive stars relative to that of  $O$ .

Table 10 is similar to Table 8 but with an extra column that gives the number of bursts,  $n$ , of each model. We did not compute a bursting SFR model for 0.1 Gyr, because the 0.1-Gyr model with continuous SFR presented in Tables 8 and 9 can be considered as a bursting model with single burst lasting 100 Myr. It can be seen from Table 10 that the  $r$  parameter is not very sensitive to  $n$ . The  $r$  parameter increases slightly as we reduce the number of bursts.

The abundance ratios for the typical irregular galaxy with bursting SFRs are given in Table 11. This Table is similar to Table 9 except for the inclusion of a new column representing the number of bursts of the model and the absence of the 0.1-Gyr model. All of the remarks drawn from Table 9 can also be drawn from Table 11; in particular, the 1.0-Gyr and 10-Gyr models reproduce well the observed  $\Delta Y/\Delta O$  value but overestimate the observed  $C/O$  and  $Z/O$  values. A slight improvement in the comparison of the predicted versus observed  $C/O$  and  $Z/O$  values is introduced by bursting SFRs (specially when  $n = 2$ ), but

TABLE 7  
CONTINUOUS SFR MODELS FOR THE TYPICAL GALAXY <sup>a</sup>

$t_g$ (Gyr)	$r$	$M_{sub}$ (%)	$M_{vl}$ (%)	$M_{rest}$ (%)	$M_{rem}$ (%)	$M_{nb}$ (%)	$\mu_{IMF}$
0.1	1.000	3.5	9.1	14.8	0.3	42.6	0.52
	1.400	13.5	14.3	17.0	0.4	25.1	0.40
	1.800	27.8	19.6	19.1	0.4	3.4	0.31
	1.855	30.1	20.3	19.4	0.5	0.0	0.30
1.0	1.000	3.1	8.2	10.6	1.2	47.2	0.56
	1.400	12.3	13.3	12.1	1.4	31.2	0.43
	1.800	25.9	18.3	14.1	1.6	10.4	0.33
	1.967	33.1	20.6	14.8	1.8	0.0	0.30
10.0	1.000	3.0	7.8	6.0	3.0	50.5	0.60
	1.400	11.6	12.5	7.0	3.5	35.7	0.46
	1.800	24.5	17.3	7.8	4.2	16.5	0.36
	2.000	32.7	19.9	8.4	4.5	4.8	0.31
	2.075	36.1	20.9	8.6	4.7	0.0	0.30

<sup>a</sup> $M_{sub} + M_{vl} + M_{rest} + M_{rem} + M_{gas} + M_{nb} = 100.0\%$ , with  $M_{gas} = 29.7\%$

TABLE 8  
ABUNDANCE RATIOS FOR THE TYPICAL GALAXY (CONTINUOUS SFRs)

$t_g$ (Gyr)	$r$	C/O	$\Delta Y/\Delta O$	Z/O
0.1	1.000	0.165	2.788	1.832
	1.400	0.166	2.873	1.855
	1.800	0.167	2.965	1.876
	1.855	0.167	2.978	1.883
	3.240 <sup>a</sup>	0.135	1.783	1.736
1.0	1.000	0.283	3.608	2.247
	1.400	0.292	3.663	2.273
	1.800	0.303	3.721	2.299
	1.967	0.307	3.747	2.315
	3.290 <sup>a</sup>	0.225	2.597	1.927
10.0	1.000	0.320	4.093	2.415
	1.400	0.322	4.130	2.427
	1.800	0.324	4.170	2.439
	2.000	0.324	4.191	2.439
	2.075	0.325	4.199	2.445
	3.390 <sup>a</sup>	0.240	2.946	1.938
Obs <sup>b</sup>		0.212	4.48	1.85
errors( $\pm$ ) <sup>b</sup>		0.071	1.02	0.20

<sup>a</sup>These lines corresponds to closed-box models from CCPS

<sup>b</sup>Taken from CCPS

TABLE 9  
BURSTING SFR MODELS FOR THE TYPICAL GALAXY <sup>a</sup>

$t_g$ (Gyr)	$n$	$r$	$M_{sub}(\%)$	$M_{vl}(\%)$	$M_{rest}(\%)$	$M_{rem}(\%)$	$M_{nb}(\%)$	$\mu_{IMF}$
1.0	2	1.930	27.5	17.6	13.2	1.6	10.4	0.33
	3	1.894	27.2	17.8	13.2	1.7	10.4	0.33
	5	1.860	26.8	18.0	13.4	1.7	10.4	0.33
	$\infty^b$	1.800	25.9	18.3	14.1	1.6	10.4	0.33
10.0	2	1.841	24.0	16.4	9.0	4.4	16.5	0.36
	3	1.832	24.2	16.7	8.4	4.5	16.5	0.36
	5	1.818	24.1	16.7	8.8	4.2	16.5	0.36
	$\infty^b$	1.800	24.5	17.3	7.8	4.2	16.5	0.36

<sup>a</sup> $M_{sub} + M_{vl} + M_{rest} + M_{rem} + M_{gas} + M_{nb} = 100.0\%$ , with  $M_{gas} = 29.7\%$

<sup>b</sup>These lines corresponds to continuous SFRs

high C/O and Z/O values continue to be predicted. Furthermore, from Figure 2 and the observed values in Table 11, it can be seen that after a burst the predicted versus the observed C/O and Z/O values become closer, but the  $\Delta Y/\Delta O$  values become farther apart.

## 7. DISCUSSION

### 7.1. The $r$ Value

The  $r$  value is almost independent of moderate changes in the high-mass limit of the IMF, alternatively it depends strongly on the low-mass limit and on the slope of the IMF at the low-mass end (see Table 1).

The average  $r(0.01, 85)$  value for the globular clusters NGC 6752 and NGC 7099 amounts to 1.85, while for  $r(0.08, 85)$  amounts to 1.32 (see Table 1). These  $r$  values are higher than those for the solar vicinity and might mean two different things: a) that the  $r$  value for the solar vicinity is not well known and that the  $r$  value for globular clusters is representative of the solar vicinity, or b) that systems with lower metallicity have higher  $r$  values. In this discussion we have not considered NGC 6397 due to the possible selective loss of low-mass stars by evaporation and tidal encounters.

A system with  $r > 1$  has a larger mass fraction of objects with  $m < 0.5$  than a system with  $r = 1$ , this is true for any value of  $m_l < 0.5$ , including the case when  $M_{sub} = 0.0$ .

### 7.2. Model Results

We have computed closed-box models for NGC 1560 and II Zw 33 that match the observed O and  $\mu_{IMF}$  values. For the 10 Gyr models the  $r$  values are equal to 1.73 and 2.75, respectively.

If the IMF is universal it follows that the same  $r$  should apply to all galaxies. From globular clusters it is obtained that  $r \sim 1.8$ , this is the best  $r$  determination available and it might apply to all galaxies.

Since closed-box models with continuous SFRs and  $M_{nb} = 0.0$  yield  $2.5 < r < 2.75$  for II Zw 33, we decided to compute other types of models with  $r = 1.8$  for this galaxy.

The closed-box continuous SFR models with  $r = 1.8$  require that  $28\% < M_{nb} < 37\%$ , in contradiction with the results of  $M_{nb} = 0.0$  derived by Walter et al. (1997). O-rich continuous SFR models with  $r = 1.8$  and  $M_{nb} = 0.0$  imply C/O > 0.383 for models older than 1.0 Gyr. This C/O value is higher than the highest value detected for an irregular galaxy (0.248 for 30 Doradus in LMC) and considerably higher than 0.158, the average C/O value for the eight irregular galaxies for which C/O is known (Garnett et al. 1995, 1997, Kobulnicky et al. 1997). The C/O values for II Zw 33 is not known and conceivable could be considerably higher than those of other irregular galaxies but it seems unlikely.

We have also computed closed-box models with continuous SFRs for the typical irregular galaxy that match the observed  $\mu$ , O, and  $\Delta Y/\Delta O$  values for different  $r$  values (see Tables 8 and 9). To choose one of these models we need to know the  $r$  or the  $M_{nb}$  value. Based on the models for NGC 1560 and on the  $r$  values for globular clusters we consider that the best models should be around  $r = 1.8$ .

A maximum value of  $r = 2.1$  is obtained when  $M_{nb} \rightarrow 0.0$  for the typical irregular galaxy (see Table 8).

We do not know which is the behavior of the IMF for  $m < 0.1$ , nor the value of  $r$ , but by assuming that  $\alpha_1$  is the same down to  $m = 0.01$ , the solution for the typical irregular galaxy with  $r(0.01, 85) = 1.80$  at 10 Gyr implies that  $M_{sub} = 24.5\%$  and  $M_{nb} = 16.5\%$ . If  $M_{sub}$  is smaller than that obtained from a given  $\alpha_1$ , it is possible to obtain a closed-box model that fits the same observational constraints by increasing  $M_{nb}$  (see Table 8).

We consider that O-rich outflows are not very important for the typical irregular galaxy because O-rich outflow models predict higher C/O and Z/O values than those observed.

The changes in the final abundance ratios between the 0.1-Gyr and the 1.0-Gyr models (see Table 9) are more important than the changes between different SFR histories, for a given  $t_g$  (see Table 11). For  $1.0 \text{ Gyr} \leq t_g \leq 10 \text{ Gyr}$  the changes between bursting and continuous SFR models are very small (see Table 11). For  $t_g = 0.1 \text{ Gyr}$ , the

TABLE 10  
ABUNDANCE RATIOS FOR THE TYPICAL GALAXY (BURSTING SFRs)

$t_g$ (Gyr)	$n$	$r$	C/O	$\Delta Y/\Delta O$	Z/O
1.0	2	1.930	0.289	4.024	2.349
	3	1.894	0.304	3.943	2.349
	5	1.860	0.319	3.894	2.358
	$\infty^a$	1.800	0.303	3.721	2.299
10.0	2	1.841	0.291	4.355	2.389
	3	1.832	0.303	4.288	2.406
	5	1.818	0.309	4.171	2.408
	$\infty^a$	1.800	0.324	4.170	2.439
Obs <sup>b</sup>			0.212	4.48	1.85
errors( $\pm$ ) <sup>b</sup>			0.071	1.02	0.20

<sup>a</sup>These lines corresponds to continuous SFRs

<sup>b</sup>Taken from CCPS

continuous SFR model can be considered as a single-burst model and the differences between this model and those for 1.0 Gyr and 10 Gyr are very significant (see Table 9).

We also consider that outflow of well-mixed material is not important. Outflow models of well-mixed material will have lower  $r$  and  $M_{sub}$  values than those presented in Tables 4, 5, 8, and 10; but to produce drastic reductions in  $r$  these models require the ejection of large amounts of gas to the intergalactic medium, that have not yet been observed around irregular galaxies. The previous discussion is based on CCPS models for outflow of well-mixed material; their models were made for  $r = 1$  while their closed-box model for 10 Gyr gives  $r = 3.39$ , and the ratio of the ejected mass to the mass left in the galaxy is 7.95.

Furthermore, in general infall of material with pregalactic abundances,  $Y = Y_p$  and  $Z = 0$ , is not important because these models are not able to match low O values with moderately low  $\mu_{IMF}$  values (Peimbert et al. 1994).

### 7.3. CCPS O-rich Outflow Models

Are the closed-box models presented in Tables 8-11 the only possibility to adjust the observational constraints of the typical irregular galaxy? The answer is no. By using the yields by Maeder (1992) CCPS have shown that it is also possible to adjust the observational constraints by means of O-rich outflow models.

The two reasons given by CCPS to support O-rich outflow models were the high  $r$  and the low  $\Delta Y/\Delta O$  values predicted by the closed-box models; for the 10 Gyr model these values amount to 3.390 and 2.946, respectively (see Table 9). This CCPS model was made under the  $M_{nb} = 0.0$  assumption. Our 10-Gyr closed-box model for the typical irregular galaxy with  $M_{nb} = 0.0$  yields  $r = 2.075$ , and  $\Delta Y/\Delta O = 4.199$ . The differences between our model and the CCPS model are only due to differences in the adopted yields.

By introducing  $M_{nb}$  values different from zero in the

CCPS models it is possible to reduce  $r$  to a reasonable value for a closed-box model; but  $\Delta Y/\Delta O$  would still be lower than observed because it is almost independent of  $r$ .

## 8. CONCLUSIONS

The IMF from globular clusters has a larger fraction of low-mass stars, and consequently a larger value of  $r$ , than the KTG IMF. This result is based on the assumption that the IMF slopes for  $m > 0.5$  are the same for all objects. The difference in the  $r$  value, if real, could be due to the lower metallicity of the globular clusters relative to the solar vicinity. Alternatively, considering that the IMF seems to be metallicity independent at higher masses, the difference in the  $r$  value could be due to observational errors; since the accuracy of the IMF determination for globular clusters is higher than for the solar vicinity maybe the lower end of the KTG IMF should be modified to agree with that derived from globular clusters.

The  $r$  values required by the closed-box models based on the yields by WLW & WW for NGC 1560 and II Zw 33, where  $M_{nb}$  has been determined, are considerably higher than one. Moreover, the  $r$  value for NGC 1560 is very similar to those derived from globular clusters.

The models based on the yields by WLW & WW predict lower  $r$  values than those based on the yields by Maeder (1992). For a given model that fits  $\mu_{IMF}$  and O, the yields by WLW & WW predict higher C/O,  $\Delta Y/\Delta O$ , and Z/O values than the yields by Maeder. The closed-box models with continuous SFRs based on the yields by WLW & WW can fit the observational constraints provided by the well observed irregular galaxies. In other words, the O-rich outflows that are required by the yields of Maeder to fit the typical irregular galaxy are not required by the yields of WLW & WW.

For models with the same age the C/O,  $\Delta Y/\Delta O$ , and Z/O ratios are almost independent of the  $r$  value.

The fit between the C/O and Z/O ratios predicted by

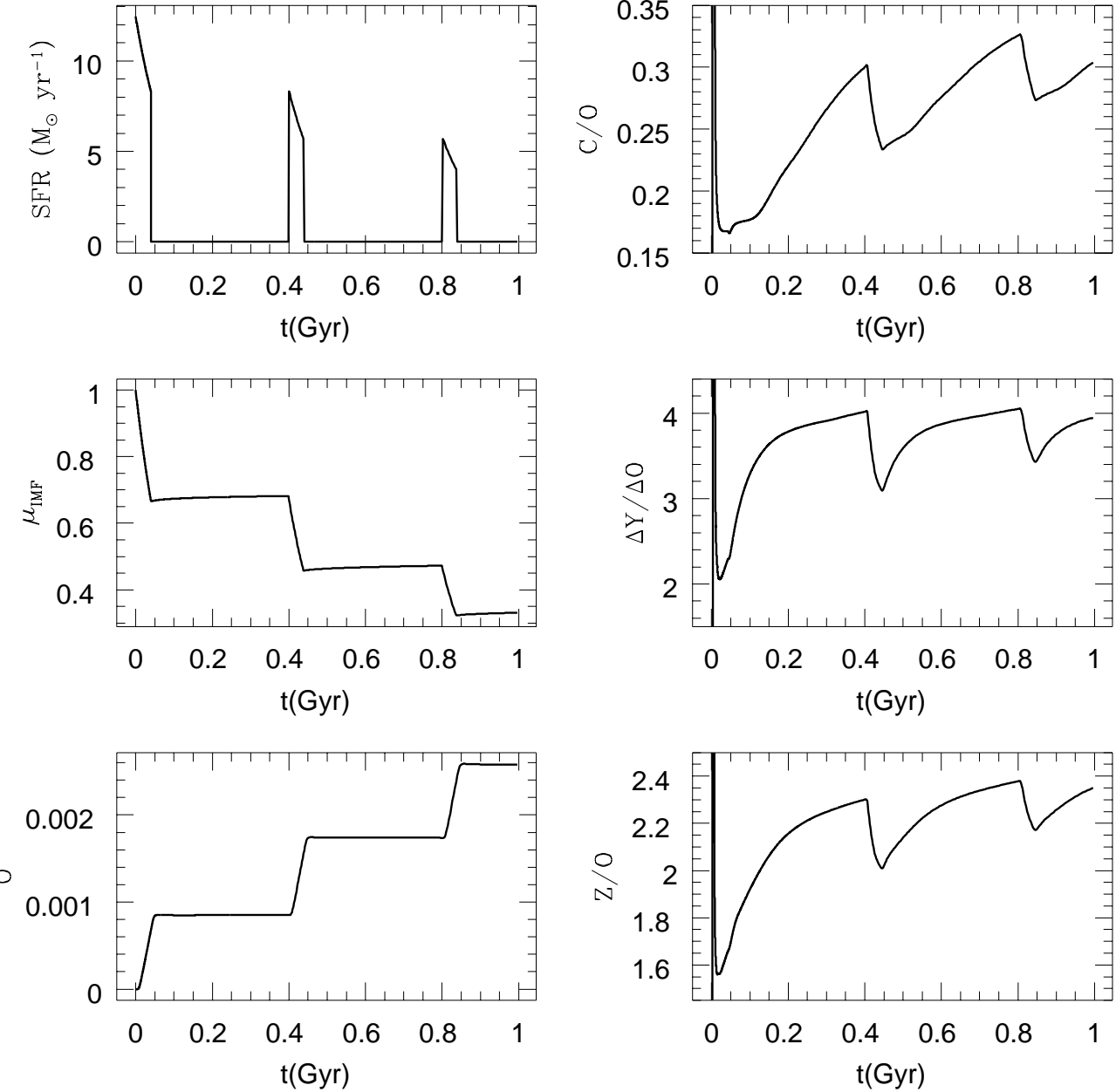


FIG. 2.— Bursting SFR model for the typical irregular galaxy with  $t_g = 1.0$  Gyr,  $n = 3$ , and  $r(0.01, 85) = 1.894$  (see Table 11). C, O, Y, and Z are given by mass.

the closed-box models with continuous SFRs and the observational constraints is only fair.

It is possible to obtain lower  $r$  values by adopting: a) O-rich outflow models or b) closed-box models with higher  $M_{nb}$  values and lower  $M_{sub}$  values (see Table 5). Nevertheless, O-rich outflow models can be disregarded for the typical irregular galaxy because they predict higher C/O and Z/O values than closed-box models and consequently

larger differences with the observed values.

A C/O determination and a better determination of  $\mu_{IMF}$  is needed for II Zw 33 to be able to discriminate among the different models that we have computed for this object.

The dark matter mass fraction for the models computed in this paper amounts to about 40%, part could be baryonic (substellar) and part non baryonic. This re-

TABLE 11  
MODELS FOR II ZW 33<sup>a</sup>

$t_g$ (Gyr)	$r$	$\gamma$	$M_{sub}(\%)$	$M_{vl}(\%)$	$M_{rest}(\%)$	$M_{rem}(\%)$	$M_{nb}(\%)$	$\mu_{IMF}$
0.1	2.502	0.00	38.6	17.7	14.6	0.3	0.0	0.29
	1.800	0.00	17.6	12.4	12.5	0.3	28.4	0.41
	1.800	0.29	29.5	20.8	20.4	0.5	0.0	0.29
1.0	2.632	0.00	41.0	17.7	11.2	1.3	0.0	0.29
	1.800	0.00	16.2	11.4	8.7	1.0	33.9	0.44
	1.800	0.33	30.7	21.7	16.8	2.0	0.0	0.29
10.0	2.750	0.00	43.3	17.8	6.6	3.5	0.0	0.29
	1.800	0.00	15.4	10.9	5.3	2.6	37.0	0.46
	1.800	0.38	32.3	22.8	10.5	5.6	0.0	0.29

<sup>a</sup> $M_{sub} + M_{vl} + M_{rest} + M_{rem} + M_{gas} + M_{nb} = 100.0\%$ , with  $M_{gas} = 28.8\%$

sult implies that  $M_{sub}$  is smaller than about 40% and that the mass fraction of non baryonic dark matter inside the Holmberg radius is also smaller than about 40%. For  $r = 1.85$ , the  $r$  value derived from globular clusters, it follows that for the typical irregular galaxy  $M_{sub} = 26.6\%$  and  $M_{nb} = 13.6\%$  inside  $R_H$ .

By comparing bursting SFR models with continuous SFR models of the same age the differences in the final abundance ratios are very small. Consequently, it can be said that the shape of the SFR does not affect the results considerably. The largest differences occur just after a burst: the C/O,  $\Delta Y/\Delta O$ , and Z/O values decrease, diminishing the differences of C/O and Z/O with the observed values but increasing the differences of the  $\Delta Y/\Delta O$

with observed value.

Manuel Peimbert acknowledges several illuminating discussions with Evan Skillman and Gerry Gilmore during the Symposium on Cosmic Chemical Evolution held in NORDITA to honor Professor Bernard Pagel. We also acknowledge a thorough reading of an earlier version of this paper and several excellent suggestions by the referee Mario Mateo. We made use of the NASA/IPAC Extragalactic Database (NED) which is operated by the Jet Propulsion Laboratory, California Institute of Technology, under contract with the National Aeronautics and Space Administration. This work was partially supported by DGAPA/UNAM through project IN-100994.

## REFERENCES

Arimoto, N., Sofue, Y., & Tsujimoto, T. 1996, PASJ, 48, 275  
 Bajaja, E., Huchtmeier, W.K., & Klein, U. 1994, A&A, 285, 385  
 Balkowski, C., Chamaraux, P., & Weliachew, L. 1978, A&A, 69, 263  
 Brinks, E., & Klein, U. 1988, MNRAS, 231, 63  
 Broeils, A.H. 1992, A&A, 256, 19  
 Burlak, A.N. 1996, Astron. Rep., 40, 621  
 Carigi, L. 1996, Rev. Mexicana Astron. Astrofis., 32, 179  
 Carigi, L., Colín, P., Peimbert, M., & Sarmiento, A. 1995, ApJ, 445, 98 (CCPS)  
 Carigi, L., & Peimbert, M. 1998, Rev. Mexicana Astron. Astrofis., submitted  
 D'Antona, F., & Mazzitelli, I. 1995, ApJ, 456, 329  
 Esteban, C., & Peimbert, M. 1995, A&A, 300, 78  
 Esteban, C., Peimbert, M., Torres-Peimbert, S., & Escalante, V. 1998, MNRAS, 295, 401  
 Ferrano, F.R., Carretta, E., Bragaglia, A., Renzini, A., & Ortolani, S. 1997, MNRAS, 286, 1012 (FCBRO)  
 Garnett, D.R., Skillman, E.D., Dufour, R.J., Peimbert, M., Torres-Peimbert, S., Terlevich, R., Terlevich, E., & Shields, G.A. 1995, ApJ, 443, 64  
 Garnett, D.R., Skillman, E.D., Dufour, R.J., & Shields, G.A. 1997, ApJ, 481, 174  
 Gottesman, S.T., & Weliachew, L. 1972, ApJ, 12, 63  
 —. 1977, A&A, 61, 523  
 Hindman, J.V. 1967, AuJPh, 20, 147  
 Israel, F.P. 1997, A&A, 317, 65  
 Izotov, Y.I., Thuan, T.X., & Lipovetski, V.A. 1997, ApJS, 108, 1  
 Kennicutt, R.C. 1998, in The Stellar Initial Mass Function, eds. G. Gilmore & D. Howell, (San Francisco:ASP Conference Series), 1  
 Kobulnicky, H.A., Skillman, E.D., Roy, J.R., Walsh, J.R., & Rosa, M.R. 1997, ApJ, 477, 679  
 Kroupa, P., Tout, C.A., & Gilmore, G. 1993, MNRAS, 262, 545 (KTG)  
 Kunkel, W.E., Demers, S., Irwin, M.J. 1996, AAS, 188.6504.  
 Kunkel, W.E., Demers, S., Irwin, M.J., & Albert, L. 1997, ApJ, 488, L129  
 Lequeux, J. 1996, in the Interplay between Massive Star Formation, the ISM and Galaxy Evolution, eds. D. Kunth, B. Guiderdoni, M. Heydari-Malayeri, & Trinh Xuan Thuan (Editions Frontieres), 105  
 Lequeux, J., Peimbert, M., Rayo, J., Serrano, A., & Torres-Peimbert, S. 1979, A&A, 80, 155  
 Lo, K.Y., Sargent, W.L.W., & Young, K. 1993, AJ, 106, 507  
 Madden, S.C., Poglitsch, A., Geis, N., Stacey, G.J., & Townes, C.H. 1997, ApJ, 483, 200  
 Maeder, A. 1992, A&A, 264, 105  
 Maloney, P., & Black, J.H. 1988, ApJ, 325, 389  
 Mateo, M. 1998, ARA&A, 36, 435  
 Moore, B. 1994, Nature, 370, 629  
 Nomoto, K., Thielemann, F.K., & Yokoi, K. 1984, ApJ, 286, 644  
 Olive, K.A., Steigman, G., & Skillman, E.D. 1997, ApJ, 483, 788  
 Pagel, B.E.J., & Portinari, L. 1998, MNRAS, 298, 747  
 Pagel, B.E.J., & Tautvaisienė, G. 1998, MNRAS in press  
 Peimbert, M., Colín, P., & Sarmiento, A. 1994, in Violent Star Formation, ed. G. Tenorio-Tagle, (Cambridge University Press), 79  
 Peimbert, M., Torres-Peimbert, S., & Ruiz, M.T. 1992, Rev. Mexicana Astron. Astrofis., 24, 155  
 Petrosian, A.R., Boulesteix, J., Comte, G., Kunth, D., & LeCoarer, E. 1997, A&A, 318, 390  
 Piotto, G., Cool, A.M., & King, I.R. 1997, AJ, 113, 1345 (PCK)  
 Renzini, A., & Voli, M. 1981, A&A, 94, 175  
 Richer, M.G., & McCall, M.L. 1995, ApJ, 445, 659  
 Salucci, P., & Persic, M. 1997, in Dark and Visible Matter in Galaxies, eds. M. Persic, & P. Salucci (San Francisco: ASP Conference Series), 1  
 Sandage, A., & Tammann, G.A. 1975, ApJ, 196, 313

Schaller, G., Schaefer, D., Meynet, G., & Maeder, A. 1992, A&AS, 96, 269

Shostak, G.S. 1974, A&A, 31, 97

Staveley-Smith, L., Davies, R.D., & Kinman, T.D. 1992, MNRAS, 258, 334 (SDK)

Tacconi, L.J., & Young, J.S. 1987, ApJ, 322, 681

Tosi, M. 1996, ASP Conf. Ser. 98, From Stars to Galaxies: The Impact of Stellar Physics on Galaxy Evolution, eds. C. Leitherer, U.F. von-Alvensleben, & J. Huchra, (San Francisco:ASP), 299

—. 1998, preprint (astro-ph/9806266).

Walter, F., Brinks, E., Duric, N., & Klein, U. 1997, AJ, 113, 2031

Welch, D.L., McLaren, R.A., Madore, B.F., & McAlary, C.W. 1987, ApJ, 321, 162

Wilson, C.D. 1995, ApJ, 448, 97

Wilson, C.D., Welch, D.L., Reid, I.N., Saha, A., & Hoessel, J. 1996 AJ, 111, 1106.

Woosley, S.E., Langer, N., & Weaver, T.A. 1993, ApJ, 411, 823 (WLW)

Woosley, S.E., & Weaver, T.A. 1995, ApJS 101, 181 (WW)